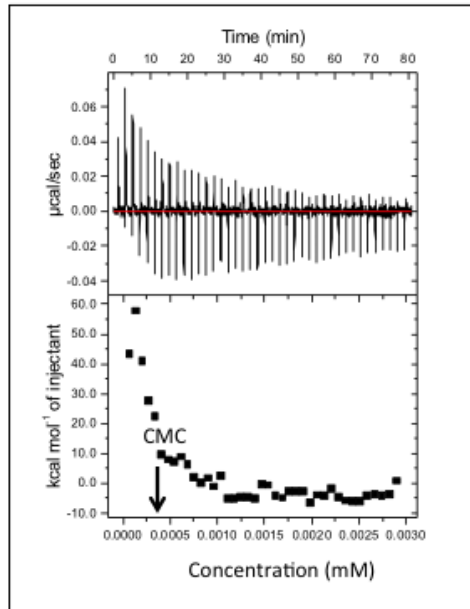
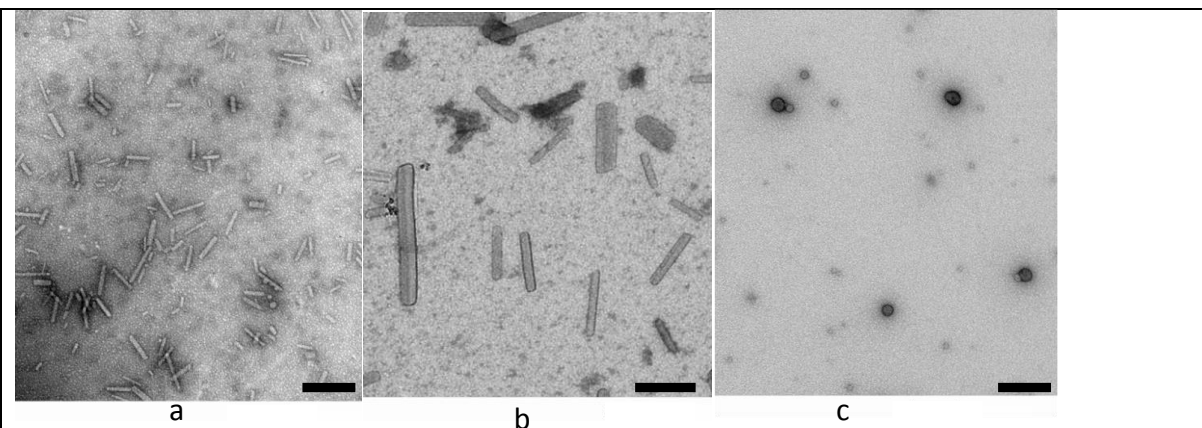


**Figure 1** Structure of *N*-(2-phenoxyacetamide)-6-*O*-glycolchitosan



**Figure 2:** Dilution enthalpogram for an aqueous dispersion of GCPH (19.35  $\mu\text{M}$ ) in water at 25  $^{\circ}\text{C}$ .



**Figure 3.** TEM images of Paclitaxel formulations: a) fine nanocrystals; b) large nanocrystals and c) GCPH nanoparticles. Scale bar = 500 nm.

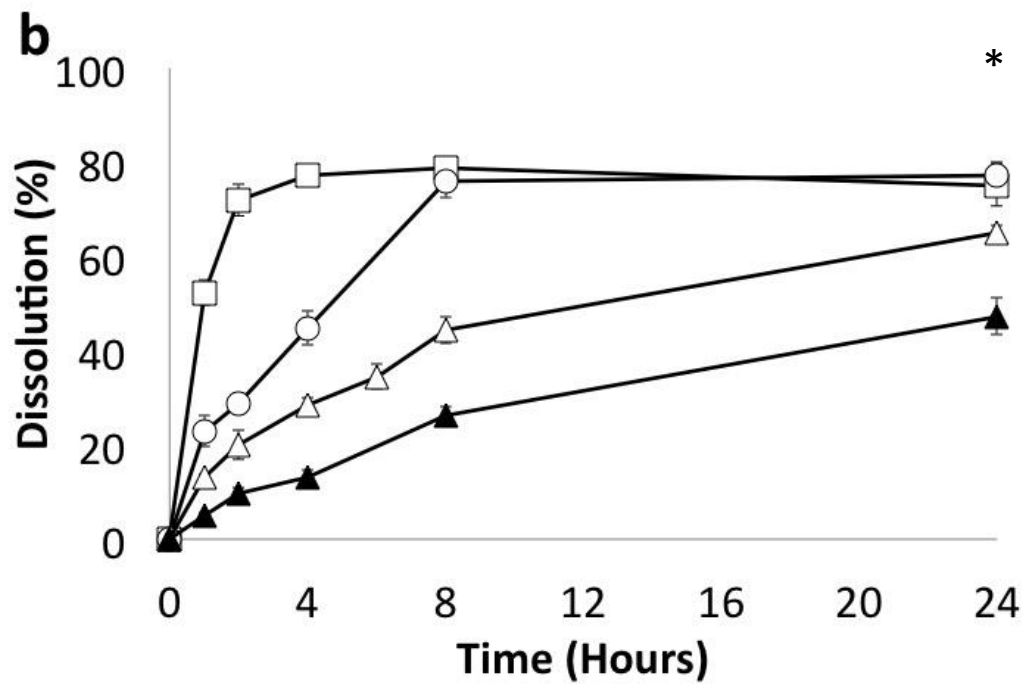
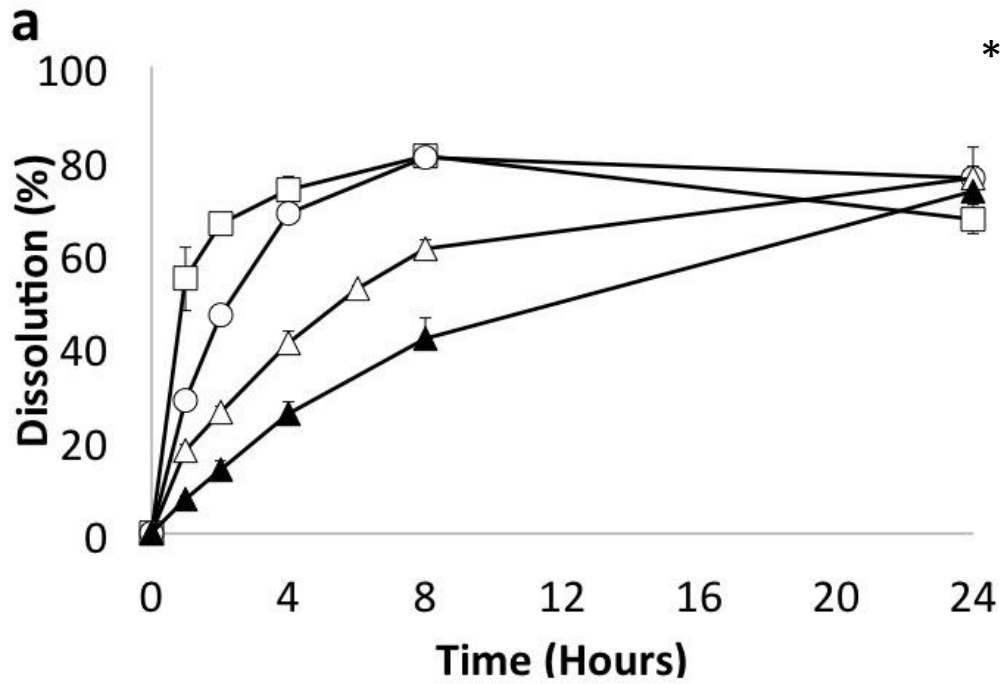


**Figure 4** Dissolution of Paclitaxel formulations (mean  $\pm$  s.d.,  $n = 3$ ,  $10 \mu\text{g mL}^{-1}$ ) in a) SGF and b) SIF.  $\square$  = GCPH - PTX,  $\circ$  = Simulated Taxol,  $\triangle$  = Paclitaxel fine nanocrystals,  $\blacktriangle$  = Paclitaxel large nanocrystals.. \*Dissolution rates from all formulations were significantly different from each other ( $p < 0.0001$ ).

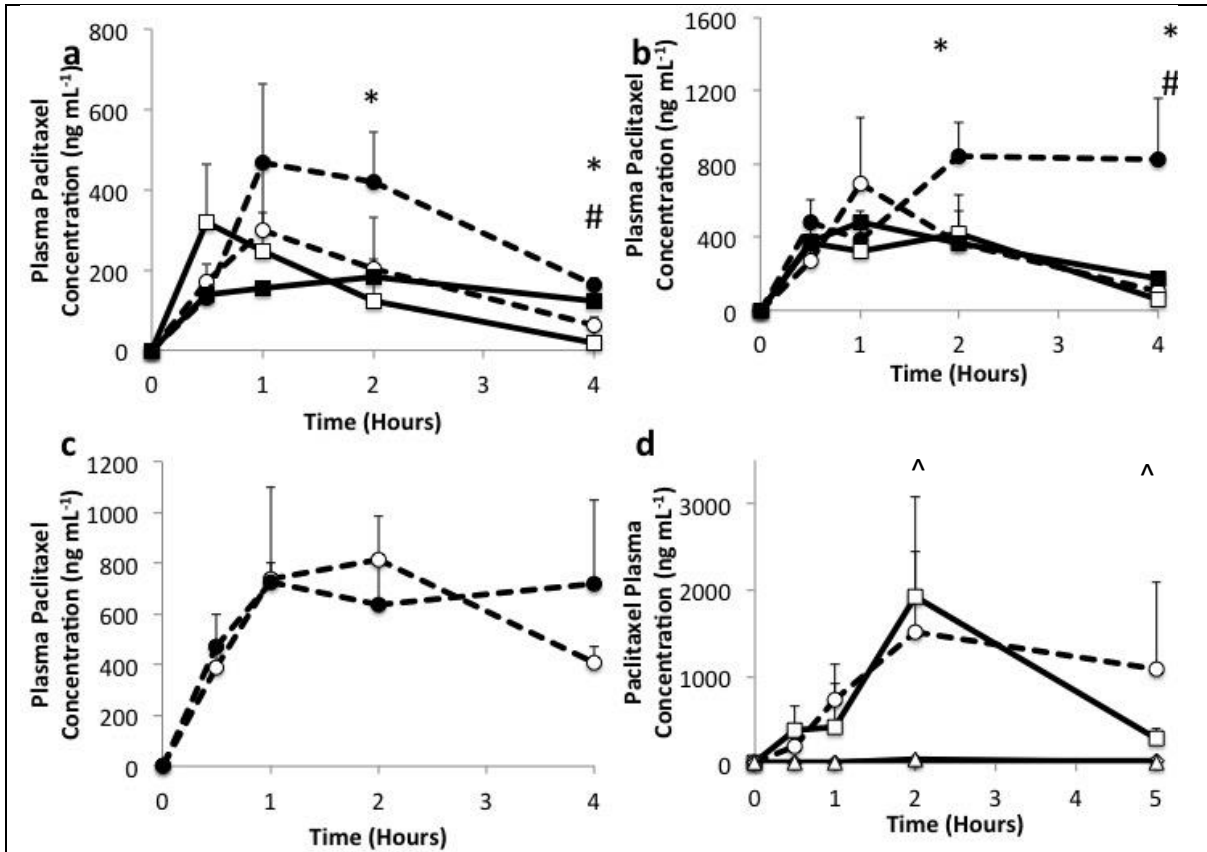


**Figure 5 a)** Plasma paclitaxel levels following the oral administration of paclitaxel formulations (mean  $\pm$  s.d., n = 3-4), open symbols = paclitaxel levels in the absence of verapamil, closed symbols = paclitaxel levels on co-administration of verapamil (40 mg kg<sup>-1</sup>): GPh-PTX = ■ □, simulated Taxol = ● ○, fine paclitaxel nanocrystals = △, large paclitaxel nanocrystals = ◇. a) = 6.7 mg kg<sup>-1</sup>, b) = 10 mg kg<sup>-1</sup>, c) = 20 mg kg<sup>-1</sup>, d) = 20 mg kg<sup>-1</sup>. \* = statistically significant difference (p < 0.05) between paclitaxel plasma levels after administration of the simulated Taxol formulation and verapamil when compared with the simulated Taxol formulation in the absence of verapamil, # = statistically significant difference (p < 0.05) between plasma levels after the administration of GPh-PTX and verapamil when compared to GPh-PTX in the absence of verapamil, ^ = statistically significant difference (p < 0.05) in plasma paclitaxel levels when the simulated Taxol and GPh-PTX formulations are compared to the crystal formulations. There were no significant differences observed between Taxol and GPh-PTX formulations themselves.

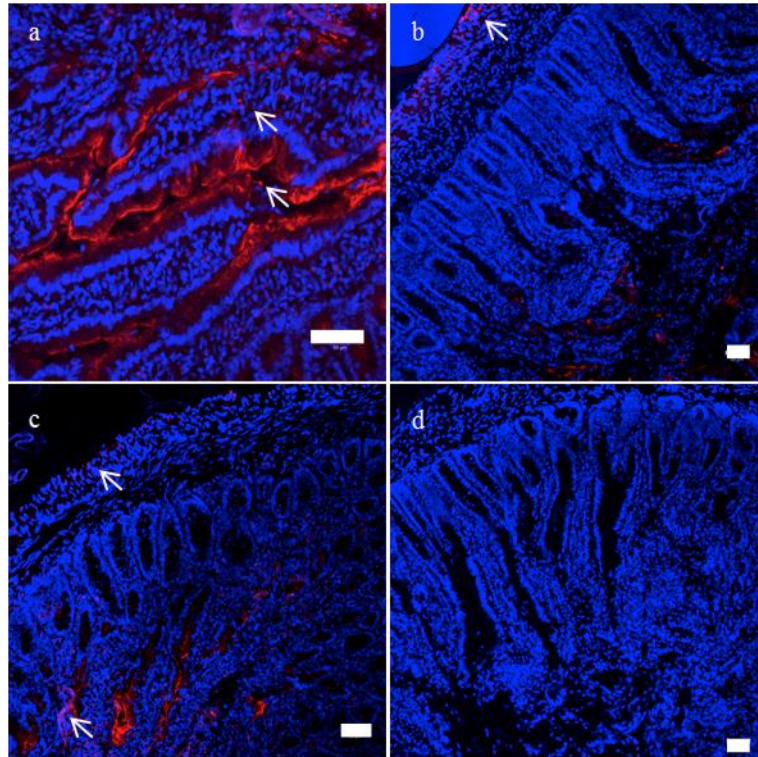


**Figure 6** Confocal laser scanning micrographs of rat intestinal tissue 2 hours after dosing with GCPH-Texas red conjugate ( $100 \text{ mg mL}^{-1}$ ). The Texas red signal (red) can be seen lining the villi (a), inside the villi and also in the basolateral side of the villi (b,c) as indicated by the arrows. (d) Blank rat intestine for comparison. (scale bars =  $10 \text{ }\mu\text{m}$ ).

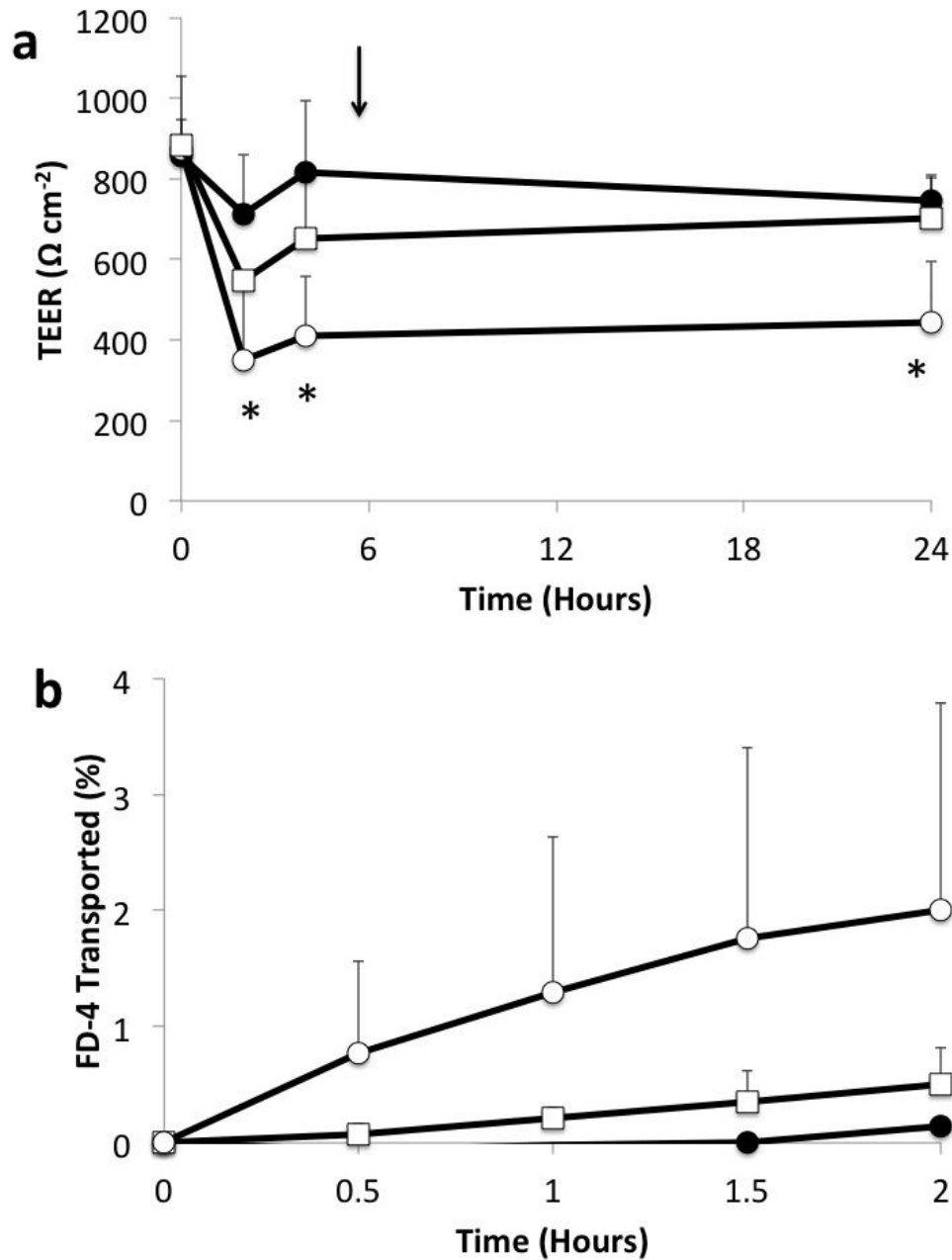


**Figure 7:** GCPH permeability enhancement across Caco-2 cell monolayers (mean  $\pm$  s.d.,  $n = 3$ , FD-4 transport in Hank's Buffered Salt Solution –  $n = 2$ ). a) The effect of GCPH ( $1\text{mg mL}^{-1}$ ) on the transepithelial resistance across a Caco-2 cell monolayer. GCPH nanoparticles =  $\circ$ , *N,N,N*-trimethylchitosan ( $1\text{mg mL}^{-1}$ , TMC) =  $\square$ , Hanks buffered salt solution (HBSS, pH 6.8) =  $\bullet$ . \* = statistically significant difference ( $p < 0.01$ ) between GCPH nanoparticles and the control (HBSS). TMC was not significant different from the buffer control. b) The transport of a paracellular marker (FD-4) across a Caco-2 cell monolayer in the presence of GCPH nanoparticles. GCPH was not significantly different from TMC.

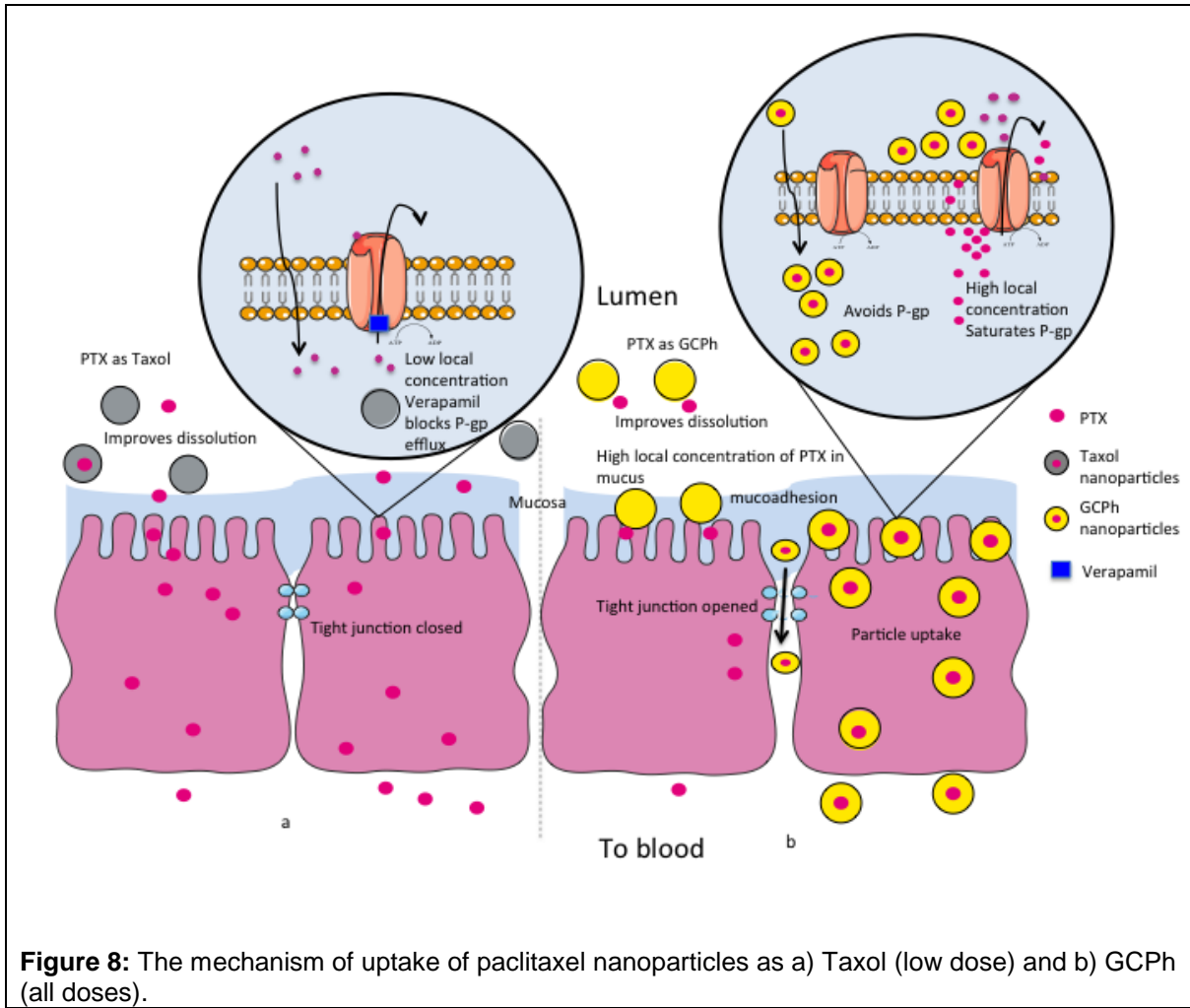


**Figure 8:** The mechanism of uptake of paclitaxel nanoparticles as a) Taxol (low dose) and b) GCPh (all doses).